

LAGRANGEAN METHOD WITH TOPOLOGICAL CHANGES FOR NUMERICAL MODELLING OF FOREST FIRE PROPAGATION

MARTIN BALAZOVJECH, KAROL MIKULA, MÁRIA PETRÁŠOVÁ, JOZEF URBÁN *

Abstract. We introduce a mathematical model and new Lagrangean numerical algorithm for modelling of a wind-driven forest fire front propagation. The model is based on evolution of plane curve (representing the fire front) in the outer normal direction by a speed given by the properties of a fuel bed which is scaled exponentially by a wind speed projected onto the normal to the front. The influence of the front shape on the speed of propagation is modelled by adding the curvature regularization to the normal velocity. For numerical modelling we use so-called Lagrangean approach where the crucial point is an asymptotically uniform tangential redistribution of grid points which prevents the moving front from forming spurious crossovers and swallow tails. Moreover, thanks to the uniform tangential redistribution and our new idea of computing distance function in a narrow tube along discrete curve grid points, we detect and solve in $O(n)$ complexity the topological changes in moving front. Such approach makes our Lagrangean method highly efficient and represents significant improvement of the existing numerical models for the forest fire propagation and, in general, it represent new fast and stable method for solving free boundary problems modelled by moving fronts with possible topological changes.

Key words. forest fire propagation, geometric partial differential equations, evolving plane curves, numerical solution, topological changes, Lagrangean approach, tangential redistribution

AMS subject classifications. 35K61, 65M08, 65Y20

1. Introduction. In this paper we present a new wind-driven forest fire propagation model and its efficient and robust numerical solution by the so-called Lagrangean approach. The proposed mathematical model has the form of an intrinsic advection-diffusion equation with a driving force which represents the equation of motion in normal direction for a closed planar curve representing the fire front. The normal velocity is influenced by the fuel bed, wind velocity and by the shape of the front represented by the local curvature. We allow topological changes in the fire front movement and present new approach for their detection and resolution. For the numerical solution we use the so-called direct Lagrangean approach where the curve is directly discretized and moved in a stable way by incorporating a suitable tangential velocity which keeps numerical grid points uniformly distributed. This property is crucial for building a stable numerical algorithm preventing the moving curve from spurious swallow tails and crossovers and also for the fast detection and resolution of topological changes during the front evolution. Our new method for treatment of topological changes has computational complexity $O(n)$, where n is a number of grid points representing the moving fire front, while standard approaches has complexity $O(n^2)$, thus the new method brings high improvement into the Lagrangean computational approaches allowing topological changes. Our spatial and temporal discretizations are based on flowing finite volume method in space and semi-implicit discretization in time. The solvability of the arising cyclic tridiagonal linear systems for any choice of

*Department of Mathematics, Slovak University of Technology, Radlinského 11, 813 68 Bratislava, Slovak Republic (balazovjech@math.sk, mikula@math.sk, jozo.urban@gmail.com) and Institute of Botany, Slovak Academy of Sciences Bratislava, Slovak Republic (maria.petrasova@savba.sk).

This work was supported by grants VEGA 1/0269/09 and APVV-0184-10.

time step is guaranteed by using the so-called inflow-implicit/outflow-explicit scheme for intrinsic advection corresponding to a tangential redistribution. It also guarantees the choice of common time step for multi-component fire front when other approaches would either lead to necessity to use different time steps (given by solvability and stability conditions) for different curves arising after a topological change or to use the smallest uniform time step for all the curves which would deteriorate both speed and precision. From all these points of view the Lagrangean numerical method which is proposed in this paper seems to be optimal with respect to stability, precision and computational complexity for a general 2D moving fronts.

Concerning the current forest fire propagation numerical models, the best known and most widely used is software FARSITE (Fire Area Simulator) described in [2]. In FARSITE, the moving fire front is given by a closed polygonal curve and its propagation is governed by the Huygens principle. It means that any point of the curve at time t is a source of an independent elliptical ignition and thus expansion [9] and new front position is constructed as an envelope of such ellipses. The half-axes of every ellipse in a point of the front depends on the local fuel bed properties and on the wind direction. There are several deficiencies in existing forest fire simulators based on evolving polygons. A first one is that the moving curve (fire front) can artificially selfintersect (or form crossovers) either due to a numerical instability in solving corresponding ODE systems or by the fact that front is coming to a time moment where a topological change should occur, cf. Figure 2.3 in section on topological changes. A treatment of topological changes, i.e. splitting and merging of moving fire front, is a nontrivial task itself, as well. In current simulation softwares it is done by testing pairwise distances of not-neighboring linear segments of the polygon [2] or by pairwise comparison of not-neighbouring grid point distances [1]. The computational complexity of such approach is proportional to the squared number of grid points representing a discrete moving front and thus the testing whether a topological change should occur takes a substantial part of computational time of the corresponding algorithm. It is worth to note that occurrence of a topological change is a rare event in general, but it must be checked at every discrete time step and thus such methods waste too much of CPU time. We cite here the FARSITE manual which states explicitly the above mentioned difficulties:

These crossovers, however, must be removed to preserve the meaningful portions of the fire front.

...a list of pairwise comparisons is made to detect intersections between each perimeter segment and every other perimeter segment of a given fire polygon.

Regardless of the methods chosen, the process of crossover removal is expensive in time and computing power, and is an interesting area for further research and improvement.

In our paper we design the Lagrangean method without such deficiencies. The presented method is fast, stable and thus robust and applicable in real-time simulations. Our work has been motivated by a cooperation with Slovak state forestry company Vojenské lesy a majetky SR, Malacky, which takes care about the forest area in the Záhorská nížina lowland, an area north-west of Bratislava, Slovakia, and has to prevent the mostly pine forests from fires which are not a rare event. The rest of the paper is organized as follows, in section 2 we describe our new Lagrangean scheme including topological changes for general curve evolution equations, in section 3 we present our model for the forest fire propagation and in section 4 we present results of numerical simulations.

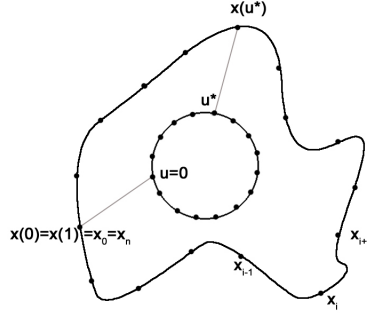


FIGURE 2.1. Curve discretization corresponding to uniform discretization of circle with unit length.

2. Lagrangean numerical algorithm. Let Γ be the plane curve, $\Gamma : S^1 \rightarrow \mathbf{R}^2$, parametrized by $u \in S^1$, where S^1 is a circle with unit length, thus $u \in [0, 1]$ and $\Gamma = \{\mathbf{x}(u), u \in S^1\}$, where $\mathbf{x}(u)$ is position vector of the curve Γ for parameter u . In our Lagrangean method the curve will be discretized as displayed in Figure 2.1, where $\mathbf{x}_0, \mathbf{x}_1, \dots, \mathbf{x}_n$ are discrete curve points which correspond to the uniform discretization of the unit circle with step $h = 1/n$ and $\mathbf{x}_0 = \mathbf{x}_n$. Let $g = |\mathbf{x}_u| > 0$ and denote by s the unit arc-length parametrization of the curve Γ . Then $ds = gdu$. The unique definition of the unit tangent \mathbf{T} and normal \mathbf{N} vectors to the plane curve Γ can be done as follows: $\mathbf{T} = \mathbf{x}_s$, $\mathbf{N} = \mathbf{x}_s^\perp$ and $\mathbf{T} \wedge \mathbf{N} = 1$, where $\mathbf{T} \wedge \mathbf{N}$ denotes the determinant of the matrix with columns \mathbf{T} and \mathbf{N} . We note that for the closed curve parametrized in a counterclockwise direction (as plotted in Fig. 2.1) such defined \mathbf{N} represents the inner unit normal vector. The motion of any point on the curve can be decomposed into the normal and tangential directions. Although it is well-known that the tangential motion does not change the shape of the evolving curve, on the other hand we know that it is helpful in stabilization of the numerical algorithms based on the Lagrangean approaches. So we consider a general form of the curve evolution in the form

$$\mathbf{x}_t = \beta \mathbf{N} + \alpha \mathbf{T}. \quad (2.1)$$

where $\beta = w + \varepsilon k$ is a velocity in the inward normal direction and α is a "free" parameter, which can be suitably chosen. From the Frenet-Serret formula we have $\mathbf{T}_s = k\mathbf{N}$, where k is the curvature, from which it follows $k\mathbf{N} = \mathbf{T}_s = (\mathbf{x}_s)_s = \mathbf{x}_{ss}$. The equation (2.1) thus can be written in the form of the following intrinsic PDE

$$\mathbf{x}_t = \varepsilon \mathbf{x}_{ss} + \alpha \mathbf{x}_s + w \mathbf{x}_s^\perp, \quad (2.2)$$

for the curve position vector $\mathbf{x} = (x_1, x_2)$. The model (2.2) is a system of two equations for the components of the position vector x_1 and x_2 . The curvature term represents the intrinsic diffusion along the curve, the tangential velocity term represents the intrinsic advection along the curve and the external driving force in the inner normal direction is given by the third term of the right hand side of (2.2).

2.1. Suitable choice of tangential velocity. In order to derive tangential velocity we follow [6, 7, 8]. We know that for any evolving curve satisfying (2.1) with arbitrary parameters α and β we get the formula which describes the evolution of

its local length $g_t = -gk\beta + g\alpha_s = -gk\beta + \alpha_u$. On the other hand, by integrating this equation along the curve we get equation for evolution of the total curve length $L_t = -L\langle k\beta \rangle_\Gamma$ where $\langle k\beta \rangle_\Gamma = \frac{1}{L} \int_\Gamma k\beta ds$ is the mean value of $k\beta$ along the curve Γ . Let us consider a numerical discretization of the ratio

$$\frac{g}{L} \approx \frac{\frac{|\mathbf{x}_i - \mathbf{x}_{i-1}|}{h}}{L} = \frac{|\mathbf{x}_i - \mathbf{x}_{i-1}|}{Lh} = \frac{|\mathbf{x}_i - \mathbf{x}_{i-1}|}{\frac{L}{n}},$$

where the numerator denotes distance between two neighbouring points and denominator a distance of neighbouring points if the curve would be uniformly discretized (since n denotes the total number of curve points and its segments). We can simply see that one can get the curve with uniformly redistributed discrete grid points if such ratio $\frac{|\mathbf{x}_i - \mathbf{x}_{i-1}|}{\frac{L}{n}} \rightarrow 1$ for all discrete segments representing distances between neighbouring points, so in the continuous formulation we should have $\frac{g}{L} \rightarrow 1$ with increasing time. By using the above results for g_t and L_t we obtain

$$\left(\frac{g}{L}\right)_t = \frac{g}{L}(-k\beta + \alpha_s + \langle k\beta \rangle_\Gamma)$$

On the other hand, we can consider e.g. the function $\frac{g}{L}(t) = 1 + \frac{g}{L}(0)e^{-\omega t}$ for which $\lim_{t \rightarrow \infty} \left(\frac{g}{L}\right) = 1$ with parameter ω controlling how fastly the redistribution becomes uniform. Such function is solution of differential equation

$$\left(\frac{g}{L}\right)_t = \omega \left(1 - \frac{g}{L}\right) \quad (2.3)$$

If we take into account both (2.3) and (2.3) we obtain differential equation

$$\alpha_s = k\beta - \langle k\beta \rangle_\Gamma + \omega \left(\frac{L}{g} - 1\right) \quad (2.4)$$

for tangential velocity α which guarantees the asymptotically uniform redistribution of grid points.

2.2. Numerical discretization of intrinsic PDE. Let us consider our general intrinsic differential equation (2.2) and integrate it on the segment $[\mathbf{x}_{i-\frac{1}{2}}, \mathbf{x}_{i+\frac{1}{2}}]$, where $\mathbf{x}_{i-\frac{1}{2}}$ denotes the middle point between the points \mathbf{x}_{i-1} and \mathbf{x}_i , i.e. $\mathbf{x}_{i-\frac{1}{2}} = \frac{\mathbf{x}_{i-1} + \mathbf{x}_i}{2}$:

$$\int_{\mathbf{x}_{i-\frac{1}{2}}}^{\mathbf{x}_{i+\frac{1}{2}}} \mathbf{x}_t ds = \varepsilon \int_{\mathbf{x}_{i-\frac{1}{2}}}^{\mathbf{x}_{i+\frac{1}{2}}} \mathbf{x}_{s,s} ds + \int_{\mathbf{x}_{i-\frac{1}{2}}}^{\mathbf{x}_{i+\frac{1}{2}}} \alpha \mathbf{x}_s ds + \int_{\mathbf{x}_{i-\frac{1}{2}}}^{\mathbf{x}_{i+\frac{1}{2}}} w \mathbf{x}_s^\perp ds.$$

Let us denote by $h_i = |\mathbf{x}_i - \mathbf{x}_{i-1}|$ the length of the linear approximation of the i -th discrete curve segment. Then we have $|\mathbf{x}_{i-\frac{1}{2}} - \mathbf{x}_{i+\frac{1}{2}}| = \frac{h_i + h_{i+1}}{2}$. Let us consider that ε, α and w are given by constant values ε_i, α_i and w_i on the curve segment $[\mathbf{x}_{i-\frac{1}{2}}, \mathbf{x}_{i+\frac{1}{2}}]$ around the point \mathbf{x}_i . Let us denote by m the time step numbering and by τ the length of discrete time step. Let us approximate the time derivative by the finite difference. Using the Newton-Leibniz formula and semi-implicit approach we get

$$\frac{h_i^m + h_{i+1}^m}{2} \frac{\mathbf{x}_i^{m+1} - \mathbf{x}_i^m}{\tau} = \varepsilon_i^m [\mathbf{x}_s^{m+1}]_{\mathbf{x}_{i-\frac{1}{2}}}^{\mathbf{x}_{i+\frac{1}{2}}} + \alpha_i^m [\mathbf{x}^{m+1}]_{\mathbf{x}_{i-\frac{1}{2}}}^{\mathbf{x}_{i+\frac{1}{2}}} + w_i^m ([\mathbf{x}^m]_{\mathbf{x}_{i-\frac{1}{2}}}^{\mathbf{x}_{i+\frac{1}{2}}})^\perp$$

from where

$$\frac{h_i^m + h_{i+1}^m}{2} \frac{\mathbf{x}_i^{m+1} - \mathbf{x}_i^m}{\tau} = \varepsilon_i^m [\mathbf{x}_s^{m+1}]_{\mathbf{x}_{i-\frac{1}{2}}^m}^{\mathbf{x}_{i+\frac{1}{2}}^m} + \alpha_i^m (\mathbf{x}_{i+\frac{1}{2}}^{m+1} - \mathbf{x}_{i-\frac{1}{2}}^{m+1}) + w_i^m (\mathbf{x}_{i+\frac{1}{2}}^m - \mathbf{x}_{i-\frac{1}{2}}^m)^\perp$$

and by approximating the arc-length derivative in the first bracket on the right hand side by the finite difference we obtain the fully-discrete semi-implicit flowing finite volume scheme [6, 7, 8],

$$\begin{aligned} \frac{h_i^m + h_{i+1}^m}{2} \frac{\mathbf{x}_i^{m+1} - \mathbf{x}_i^m}{\tau} &= \varepsilon_i^m \left(\frac{\mathbf{x}_{i+1}^{m+1} - \mathbf{x}_i^{m+1}}{h_{i+1}^m} - \frac{\mathbf{x}_i^{m+1} - \mathbf{x}_{i-1}^{m+1}}{h_i^m} \right) \\ &+ \alpha_i^m \left(\frac{\mathbf{x}_{i+1}^{m+1} - \mathbf{x}_{i-1}^{m+1}}{2} \right) + w_i^m \left(\frac{\mathbf{x}_{i+1}^m - \mathbf{x}_{i-1}^m}{2} \right)^\perp. \end{aligned} \quad (2.5)$$

As one can see, we have obtained two cyclic tridiagonal systems of linear equations for position vector components $\mathbf{x}_i^{m+1} = ((\mathbf{x}_i^{m+1})_1, (\mathbf{x}_i^{m+1})_2)$, where $i = 1, \dots, n$ and $\mathbf{x}_0^{m+1} = \mathbf{x}_n^{m+1}$ resp. $\mathbf{x}_{n+1}^{m+1} = \mathbf{x}_1^{m+1}$. The tangential velocity α_i^m is computed as follows. We set $\alpha_0^m = 0$, i.e. the point \mathbf{x}_0 will not be moving in tangential direction, but only in the normal direction. Then we get discretization of (2.4) in the form

$$\alpha_i^m = \alpha_{i-1}^m + h_i^m k_i^m \beta_i^m - \langle k\beta \rangle_\Gamma^m h_i^m + \omega \left(\frac{L^m}{n} - h_i^m \right) \quad (2.6)$$

where the curvature k_i^m , the normal component of velocity β_i^m , for $i = 1, \dots, n$, the mean value $\langle k\beta \rangle_\Gamma^m$ and the total length L^m are computed by using the following formulas:

$$\begin{aligned} k_i^m &= \text{sgn}(R_{i-1} \wedge R_{i+1}) \frac{1}{2h_i^m} \arccos \left(\frac{R_{i+1} \cdot R_{i-1}}{h_{i+1}^m h_{i-1}^m} \right), \\ \beta_i^m &= \frac{\varepsilon_{i-1}^m + \varepsilon_i^m}{2} k_i^m + \frac{w_{i-1}^m + w_i^m}{2}, \quad \langle k\beta \rangle_\Gamma^m = \frac{1}{L^m} \sum_{l=1}^n h_l^m k_l^m \beta_l^m, \quad L^m = \sum_{l=1}^n h_l^m, \end{aligned}$$

where $R_i = ((R_i)_1, (R_i)_2)^T = \mathbf{x}_i^{m-1} - \mathbf{x}_{i-1}^{m-1}$. The above constructed system (2.5) is cyclic tridiagonal and can be written in the following form

$$-A_i^m \mathbf{x}_{i-1}^{m+1} + B_i^m \mathbf{x}_i^{m+1} - C_i^m \mathbf{x}_{i+1}^{m+1} = D_i^m, \quad (2.7)$$

where D_i^m is right hand side and $A_i^m = -\frac{\alpha_i^m}{2} + \frac{\varepsilon_i^m}{h_i^m}$, $C_i^m = \frac{\alpha_i^m}{2} + \frac{\varepsilon_i^m}{h_{i+1}^m}$ and $B_i^m = (H_i^m + A_i^m + C_i^m)$, where $H_i^m = \frac{h_{i+1}^m + h_i^m}{2\tau}$. It can be solved by the cyclic tridiagonal solver which uses Sherman-Morrison formula in order to generalize the classical Thomas algorithm to the matrices with non-zero elements in matrix corners. As in the case of the Thomas algorithm, the solvability is guaranteed by the diagonal dominance of the system matrix. In case of (2.5) the diagonal dominance yields the condition $|B_i^m| \geq |-A_i^m| + |-C_i^m| = |A_i^m| + |C_i^m|$. Since in the semi-implicit approach the system parameters are fixed from the previous time step this condition can be fulfilled only by the proper choice of the time step τ according to the next condition

$$\tau \leq \frac{1}{2} \frac{h_{i+1}^m + h_i^m}{\left| \frac{\varepsilon_i^m}{h_i^m} - \frac{\alpha_i^m}{2} \right| + \left| \frac{\varepsilon_i^m}{h_{i+1}^m} + \frac{\alpha_i^m}{2} \right| - \left(\frac{\varepsilon_i^m}{h_i^m} + \frac{\varepsilon_i^m}{h_{i+1}^m} \right)}, \quad (2.8)$$

which must be tested for all $i = 1, \dots, n$ in every time step. Such test is time consuming itself and moreover it can give different values of τ for different curves arising e.g. after a topological change. The smallest τ then must be chosen which again slowed down the speed of this semi-implicit scheme. For this reason it is useful to modify the scheme, in order to get a method which is not constrained by the choice of the length of discrete time step.

2.3. Numerical scheme without restriction on time step. To motivate the scheme, let us consider the advection equation

$$q_t + vq_x = 0, \quad (2.9)$$

where $q : \Omega \times [0, T] \rightarrow \mathbf{R}$ is an unknown function and $v(x)$ is a scalar velocity field. We solve the equation (2.9) in a domain $\Omega \subset \mathbf{R}$ and in time interval $[0, T]$. Let us denote by p_i a finite volume (in our case it will be a segment of the curve $[\mathbf{x}_{i-\frac{1}{2}}, \mathbf{x}_{i+\frac{1}{2}}]$ around the point \mathbf{x}_i), with length h . The equation (2.9) can be rewritten as

$$q_t + (vq)_x - qv_x = 0. \quad (2.10)$$

If we integrate (2.10) on the finite volume p_i , we get

$$\begin{aligned} h(\bar{q}_i)_t + v_{i+\frac{1}{2}}\bar{q}_{i+\frac{1}{2}} - v_{i-\frac{1}{2}}\bar{q}_{i-\frac{1}{2}} - \bar{q}_i(v_{i+\frac{1}{2}} - v_{i-\frac{1}{2}}) &= 0, \\ h(\bar{q}_i)_t + v_{i-\frac{1}{2}}(\bar{q}_i - \bar{q}_{i-\frac{1}{2}}) + (-v_{i+\frac{1}{2}})(\bar{q}_i - \bar{q}_{i+\frac{1}{2}}) &= 0, \end{aligned} \quad (2.11)$$

where $v_i = v(x_i)$, $v_{i-\frac{1}{2}} = v(x_{i-\frac{1}{2}})$, $v_{i+\frac{1}{2}} = v(x_{i+\frac{1}{2}})$, and \bar{q}_i , $\bar{q}_{i-\frac{1}{2}}$ and $\bar{q}_{i+\frac{1}{2}}$ are representative values of solution inside and on the boundaries of the finite volume p_i . If $v_{i-\frac{1}{2}} > 0$, it represents the inflow into the finite volume from the left side. If $v_{i+\frac{1}{2}} < 0$, it represents the inflow to the finite volume from the right side. If the signs are opposite, they represent outflows from the finite volume. Let us define

$$\begin{aligned} b_{i-\frac{1}{2}}^{in} &= \max(v_{i-\frac{1}{2}}, 0), \quad b_{i-\frac{1}{2}}^{out} = \min(v_{i-\frac{1}{2}}, 0), \\ b_{i+\frac{1}{2}}^{in} &= \max(-v_{i+\frac{1}{2}}, 0), \quad b_{i+\frac{1}{2}}^{out} = \min(-v_{i+\frac{1}{2}}, 0). \end{aligned} \quad (2.12)$$

Let q_i be the solution of the scheme for the finite volume p_i . The representative values will be obtained from the values q_i by reconstructions $\bar{q}_{i-\frac{1}{2}} = \frac{q_i + q_{i-1}}{2}$, $\bar{q}_{i+\frac{1}{2}} = \frac{q_i + q_{i+1}}{2}$ and $\bar{q}_i = q_i$ in the inflow part while $\bar{q}_i = \frac{\bar{q}_{i-\frac{1}{2}} + \bar{q}_{i+\frac{1}{2}}}{2}$ in the outflow part. Then, let us approximate the time derivative by the finite difference and take the inflow implicitly and the outflow explicitly as suggested in [4, 5], cf. also [3]. We get the I²OE scheme in the form

$$\begin{aligned} \frac{h}{\tau} q_i^{m+1} + \frac{1}{2} b_{i-\frac{1}{2}}^{in} (q_i^{m+1} - q_{i-1}^{m+1}) + \frac{1}{2} b_{i+\frac{1}{2}}^{in} (q_i^{m+1} - q_{i+1}^{m+1}) = \\ \frac{h}{\tau} q_i^m - \frac{1}{4} \left(b_{i-\frac{1}{2}}^{out} (q_{i+1}^m - q_{i-1}^m) + b_{i+\frac{1}{2}}^{out} (q_{i-1}^m - q_{i+1}^m) \right). \end{aligned}$$

Since the velocity α_i is given in the centers of finite volumes (the points \mathbf{x}_i) and not on their boundaries and in our case of the curve evolution equation (2.2) it is on the right hand side and thus we have $v_i = -\alpha_i$, we modify the above I²OE scheme by defining

$$b_{i-\frac{1}{2}}^{in} = \max(-\alpha_i, 0), \quad b_{i-\frac{1}{2}}^{out} = \min(-\alpha_i, 0), \quad b_{i+\frac{1}{2}}^{in} = \max(\alpha_i, 0), \quad b_{i+\frac{1}{2}}^{out} = \min(\alpha_i, 0)$$

and unknowns are components of the position vector \mathbf{x}_i for which we get our final numerical scheme:

$$\begin{aligned}
& - \left(\frac{\varepsilon_i^m}{h_i^m} + \frac{1}{2} b_{i-\frac{1}{2}}^{in} \right) \mathbf{x}_{i-1}^{m+1} - \left(\frac{\varepsilon_i^m}{h_{i+1}^m} + \frac{1}{2} b_{i+\frac{1}{2}}^{in} \right) \mathbf{x}_{i+1}^{m+1} + \\
& \left(\frac{h_{i+1}^m + h_i^m}{2\tau} + \frac{\varepsilon_i^m}{h_{i+1}^m} + \frac{\varepsilon_i^m}{h_i^m} + \frac{1}{2} b_{i-\frac{1}{2}}^{in} + \frac{1}{2} b_{i+\frac{1}{2}}^{in} \right) \mathbf{x}_i^{m+1} = \quad (2.13) \\
& \frac{h_{i+1}^m + h_i^m}{2\tau} \mathbf{x}_i^m - \frac{1}{4} b_{i-\frac{1}{2}}^{out} (\mathbf{x}_{i+1}^m - \mathbf{x}_{i-1}^m) - \frac{1}{4} b_{i+\frac{1}{2}}^{out} (\mathbf{x}_{i-1}^m - \mathbf{x}_{i+1}^m) + w_i^m \left(\frac{\mathbf{x}_{i+1}^m - \mathbf{x}_{i-1}^m}{2} \right)^\perp.
\end{aligned}$$

Now, the coefficients A_i^m , B_i^m and C_i^m in corresponding system (2.7) are always non-negative, the system matrix is diagonally dominant M-matrix and thus it is always solvable by the cyclic tridiagonal solver without any restriction on time step length τ . A possible negative values of A_i^m and C_i^m in the classical system (2.7) were caused by the intrinsic advection which corresponds to the tangential velocity α . This problem is solved by our treatment of advection using the inflow-implicit/outflow-explicit splitting. This approach has the second order accuracy in space and time in case of the scalar advection equation [4, 5] and for the curve evolution model it keeps the grid points on the circle for the constantly rotating tangential velocity.

2.4. Topological changes. By the topological change we mean splitting of the evolving curve into several separate parts. Such situations can occur during the evolution mainly around nonburnable regions or when the curve velocity is slowed down significantly locally. Together with splitting, we can consider also merging of several fire fronts. Solution of such problems can be treated analogously to the approach presented here. Detecting and solving the topological changes in the Lagrangean approach is usually highly time consuming because the standard approaches has computational complexity $O(n^2)$ where n is the number of curve grid points. Such complexity is due to a standard strategy for the topological change detection which consists in computing distances between all grid points of the curve. Then, if the smallest computed distance is realized not among the neighbouring grid points and it is below a specified threshold, it indicates that the curve should be split to two curves in those points. The number of operations in such approach is $\sum_{i=2}^{n-2} (n-i) = \frac{n^2-3n}{2}$ and it slows down computing time significantly.

Our goal is to develop new method for the topological changes detection with much lower complexity. We follow the same strategy to find two not-neighbouring points with the smallest distance below some threshold. But we find this couple in completely different and fast way. Our curve is asymptotically uniformly discretized which means that all distances are close to their mean value. The global length can increase (fire front expands) or decrease (after a topological change) during the evolution. If the mean distance between neighbouring grid points is greater than 1 (the size of one pixel in the forestry (bit)map is $1m^2$, see Fig. 2.3) we densify the curve, which means that we put new point in the middle of every curve segment and thus the number of points is doubled. On the other hand, if the mean distance is less than 0.4 we coarse the discretization and remove half of the grid points. By this procedure we guarantee that for a smooth curve there are generically maximally 3 grid points in one pixel.

Our main new idea is to create a narrow strip (with thickness 1) of pixels along the curve. If there is no topological change occurring, this strip should not be crossed

by two distant pieces of the curve. On the other hand, if there are two distant points inside one pixel of this strip, it indicates the topological change. So our algorithm is as follows:

1. we traverse all curve grid points and mark the pixels in which they lie by $j = 0$.
2. we traverse again subsequently all points and ask whether the pixel value j where the point belongs is equal to 0. If yes, set it to i , where i is the number of grid point. If it is not 0, it means that the value in pixel was set by another point j . If $i - j \leq 2$ then go to another point. If $i - j > 2$ then there are more than two points between the points i and j , and i and j belong to one pixel. It is clear that such situation indicates the splitting of the curve.
3. if such splitting was detected, we do a test of distances between the sets of points $\{i - 2, i - 1, i, i + 1, i + 2\}$ and $\{j - 2, j - 1, j, j + 1, j + 2\}$. If the smallest distance is less than a given threshold (in our case the mean distance) then the curve is split in two points where this smallest distance was computed.

From the above description it is clear that the number of operations is proportional only to number of grid points and thus our algorithm has complexity $O(n)$, see also Figure 2.2.

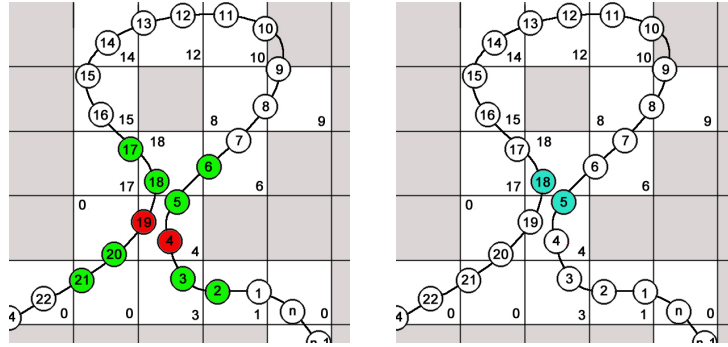


FIGURE 2.2. *Detection of topological changes. In the left figure, the points x_4 and x_{19} are detected as indicators of the topological change, they are distant but in one pixel. The smallest distance in their local neighbourhood is then computed for the points x_5 and x_{18} (right figure) where the topological change is performed and two new curves are created each of which contains x_5 and x_{18} .*

3. Fire front propagation model. We have at disposal the forestry typological maps where recorded data includes a species composition, age and density of the trees. Such data are provided in *shp* format which is then used in ArcGIS software to create a bitmap images with the resolution 1000 x 1000 pixels corresponding to area 1 x 1 km. The greyscale color of the image is given by the combustibility of an underlying forest which we get by a combination of age and density of species. Here, the black color represents a non-flammable material (river, road) and white the most burnable material (young, dense, coniferous forest). The graylevels in between thus give the local speed of fire front propagation in the range from 0 (black) to a maximal speed of fire propagation with zero wind velocity (white) which is e.g. 1 meter/minute for the young and dense pine forest. By this approach we have given the scalar velocity function f depending on the spatial position \mathbf{x} which represents the speed of linear fire front in outer unit normal direction without wind and terrain slope. The influence of the wind and terrain slope on the fire front propagation has

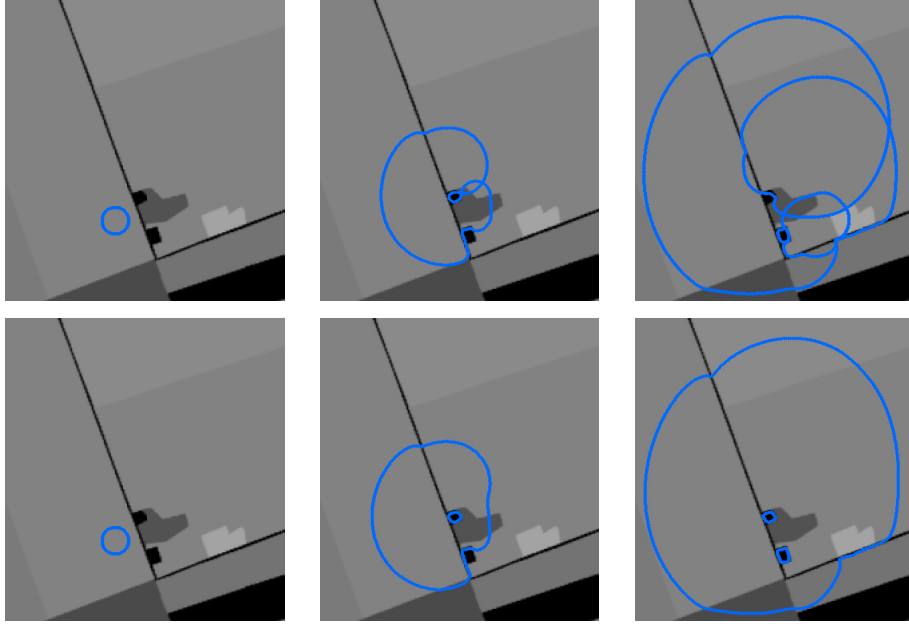


FIGURE 2.3. *Curve evolution in nonhomogeneous media by the Lagrangean approach without treatment of topological changes (up) and with treatment of topological changes (down).*

the same character. Increasing the wind speed or terrain slope in the direction of the fire front head increases the speed of front head while decreasing the front speed on its back. This can be modelled by a projection of the wind speed (or terrain slope) vector \mathbf{v} to the outer unit normal of the front ($-\mathbf{N}$) which is then an input to (e.g. exponential) function having the property to increase velocity f at the head of the front and decrease it at the back of the front. Thus we can write the equation for the inner normal velocity β considered in the previous section as follows

$$\beta = -f e^{-\lambda(\mathbf{v} \cdot \mathbf{N})}. \quad (3.1)$$

Since such inner normal velocity is always negative, the outer normal velocity is positive and the front is always expanding. It is worth to note that the choice of the exponential function with a positive parameter λ was justified in [10] for the pine forests. Both from the real observations and physical considerations related to a heat radiation which is the main driving force for the forest fire propagation it follows that there is an influence of the local shape of the front, expressed by the curvature k , on the fire front speed. If the front is convex (which means with positive curvature) then there is larger portion of unburned forest encompassing the front than in linear case, it dries slowly and thus the speed of propagation in outer normal direction is slowed down (and in inner normal direction is fasten up). In opposite, if the shape of front is concave (which means with negative curvature), the unburned forest is largely encompassed by burning area and thus the front speed in outer normal direction must be larger as in the linear case. Such situations can be modelled e.g. by modifying β in the following sense

$$\beta = -f e^{-\lambda(\mathbf{v} \cdot \mathbf{N})}(1 - \delta k), \quad (3.2)$$

which represents our final mathematical model for the forest fire front propagation. The model has two empirical parameters λ and δ which must be given by laboratory experiments or tuned in real simulations e.g. using the past forest fire records. The equation (3.2) for the inner normal velocity of the fire front is rewritten into the form of intrinsic PDE (2.2) with $\varepsilon = \delta f e^{-\lambda(\mathbf{v}\cdot\mathbf{N})}$, $w = -f e^{-\lambda(\mathbf{v}\cdot\mathbf{N})}$ and with α given by (2.4) which is then solved by the numerical scheme (2.13) and by treatment of topological changes as described in section 2.4.

4. Computational results. First, let us compare computationally our approach to topological change detection with the standard one where distances among all grid points are computed [2, 1]. We run 10000 time steps in the same wind conditions and starting at same place, cf. Fig. 2.3 bottom row. Using standard approach the computation took 709.89 seconds and the detection of topological changes took 669.16 seconds while the rest was spent in solving tridiagonal systems for updating the evolving curve(s) position. The topological change detection cover 94.26% of the whole computing time. Using our new approach the overall computation took only 44.85 seconds and the detection of topological changes took only 3.381 seconds which was only 7.53% of the whole computing time. The resulting curve evolution was same using both approaches while our new method brings high acceleration regarding CPU time. The computations have been performed on standard PC (Intel Core 2 Duo CPU 1.66 GHz, 2 GB RAM).

At the end we present computational reconstruction of the real forest fire from August 29th, 1992 which took place in the Záhorská nížina lowland. Fire began near the highway from Bratislava to Brno (the small circle in the left bottom corner of the map presented left up in Fig. 4.1) and very soon a large area of pine forest was stricken. It is known from literature that maximal velocity of fire front propagation in pine forest (without wind) is 1 meter per minute. From the records of Slovak weather forecast services (Slovenský Hydrometeorologický Ústav) we know that in that location the averaged wind velocity on August 29th, 1992 was 6 meters per second and the wind direction was 85 deg from the x axis. It is a flat area so there is no need to consider the influence of the terrain slope. By the records of fire department of Vojenské lesy a majetky SR, Malacky, we know that the fire passed in 1 day (1440 minutes) about 3 km to the lake Tančibok (indicated on the bottom right map). For the computation we use the forestry map of the region which was valid before the forest fire and we have chosen the length of time step $\tau = 0.1$ minute and the model parameters $\lambda = 0.26$, $\delta = 3$. In Fig. 4.1 we plot the fire front after 0, 5000, 10000 and 14000 time steps when the lake Tančibok was reached.

REFERENCES

- [1] P. PAUŠ, M. BENEŠ, *Algorithm for topological changes of parametrically described curves*, Proceedings of ALGORITMY 2009, pp. 176-184
- [2] M.A. FINNEY, *FARSITE: Fire Area Simulator, model development and evaluation*. Research Paper RMRS-RP-4 Revised. Ogden, UT: U.S. Department of Agriculture, Forest Service, Rocky Mountain Research Station., 2004
- [3] K. MIKULA, M. OHLBERGER, *A new level set method for motion in normal direction based on a semi-implicit forward-backward diffusion approach*, SIAM J. Scientific Computing, Vol. 32, No. 3 (2010) pp. 1527-1544.
- [4] K. MIKULA, M. OHLBERGER, *Inflow-Implicit/Outflow-Explicit Scheme for Solving Advection Equations*, Proceedings of FVCA6 conference in Prague, Springer-Verlag, Berlin, 2011.
- [5] K. MIKULA, M. OHLBERGER, J. URBÁN *Inflow-Implicit/Outflow-Explicit Finite Volume Meth-*

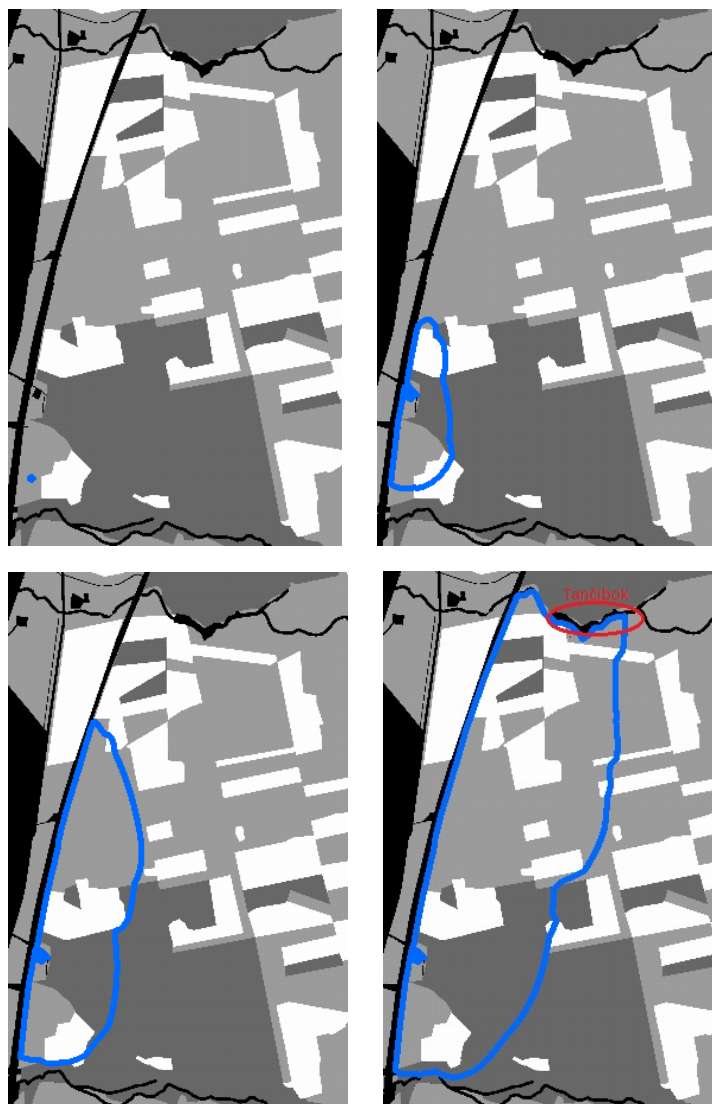


FIGURE 4.1. Real wild forest fire reconstruction, the Záhorská nížina lowland, August 29th, 1992.

- ods for Solving Advection Equations*, Technical Report 01/12 - N , FB 10 , University of Münster, February 2012
- [6] K. MIKULA, D. ŠEVČOVIČ, *Evolution of plane curves driven by a nonlinear function of curvature and anisotropy*, SIAM J. Appl. Math., 61 (2001), pp. 1473–1501.
- [7] K. MIKULA, D. ŠEVČOVIČ, *A direct method for solving an anisotropic mean curvature flow of planar curve with an external force*, Mathematical Methods in Applied Sciences, 27(13) (2004) pp. 1545-1565.
- [8] K. MIKULA, D. ŠEVČOVIČ, M.BALAŽOVJECH, *A simple, fast and stabilized flowing finite volume method for solving general curve evolution equations*, Communications in Computational Physics, Vol. 7, No. 1 (2010) pp. 195-211
- [9] G.D. RICHARDS, *An elliptical growth model of forest fire fronts and its numerical solution*, Int. J. Numer. Meth. Eng., Vol. 30 (1990) pp.1163-1179
- [10] D.X. VIEGAS, L.P. PITA, L. MATOS, P. PALHEIRO, *Slope and wind effects on fire spread*, Forest Fire Research and Wildland Fire Safety, Millpress, Rotterdam, ISBN 90-77017-72-0, 2002